

DIRECT OBSERVATION OF ORTHO-PARA TRANSITIONS IN METHANE *

Irving Ozier

Science Center, North American Rockwell Corporation, Thousand Oaks, California 91360

and

Pon-nyong Yi,† Ashok Khosla, and Norman F. Ramsey

Lyman Laboratory of Physics, Harvard University, Cambridge, Massachusetts 02138

(Received 12 February 1970)

Ortho-para transitions have been observed directly in CH₄ for the first time. These normally forbidden transitions were observed in the ground electronic, ground vibrational, and $J=2$ rotational state by combining a simple level-crossing technique with the conventional molecular-beam magnetic-resonance method. It is shown how this spectrum can be used to measure, for certain tetrahedral molecules, the interaction constants which appear in the Zeeman, nuclear-hyperfine and rotational-distortion Hamiltonians.

It is well known that H₂ has two modifications¹: parahydrogen, where the total nuclear spin $I=0$, and orthohydrogen, where $I=1$. For an isolated H₂ molecule in a homogeneous magnetic field \vec{H} , symmetry conditions forbid mixing between states corresponding to different values of I , and ortho-para transitions cannot occur. Methane, on the other hand, has three modifications: para ($I=0$), ortho ($I=1$), and meta ($I=2$). In this case, the nuclear hyperfine interactions can mix states corresponding to different values² of I , but this mixing is generally small. As a result, I is considered to be a good quantum number,²⁻⁴ and ΔI transitions in which the molecule changes from one modification to another are forbidden.

It is the purpose of the present Letter to report the direct observation of ortho-para transitions in the $J=2$ rotational level of CH₄ by the molecular-beam magnetic-resonance method.⁵ The observation of these normally forbidden transitions was made possible by setting the field \vec{H} to a value near that corresponding to a level crossing where the mixing referred to above is large. Several studies⁶ have been carried out recently on the effect of the spin conversion produced by thermal relaxation processes on various allowed spectra. However, the current work constitutes the first direct observation of ΔI transitions in CH₄. The present experiment not only provides valuable insight into the mechanisms operating in some of these relaxation processes, but also forms the basis of an accurate method of measuring (for certain tetrahedral molecules) the various interaction constants of the Zeeman, nuclear-hyperfine and rotational-distortion Hamiltonians.

The specific system we shall be concerned with here is an isolated CH₄ molecule in its

ground electronic and vibrational state and $J=2$ rotational state which has been placed in a homogeneous magnetic field \vec{H} pointing in the Z direction. For this system, the effective Hamiltonian can be written^{2-4,7-9}

$$W = B_0 \vec{J}^2 - D_U O_{\text{dist}}^{(3)} - D_T O_{\text{dist}}^{(4)} - g_I (\mu_N / h) I_Z H - g_J (\mu_N / h) J_Z H - c_a \vec{I} \cdot \vec{J} - \frac{1}{3} c_d O_{\text{sr}} + \frac{3}{16} d O_{\text{ss}}. \quad (1)$$

The first three terms form⁷ the rotational Hamiltonian W_{rot} . $B_0 \vec{J}^2$ is the energy of rigid rotation, while the second and third terms result from centrifugal distortion effects.⁷ $O_{\text{dist}}^{(3)}$ and $O_{\text{dist}}^{(4)}$ are third- and fourth-rank tensors, respectively, which are constructed from the components of \vec{J} so as to transform by representation A_1 of the point group T_d .

$$O_{\text{dist}}^{(3)} \equiv i \{ [\tilde{J}_Z \tilde{J}_-^2 + \tilde{J}_-^2 \tilde{J}_Z] - [\tilde{J}_Z \tilde{J}_+^2 + \tilde{J}_+^2 \tilde{J}_Z] \}, \quad (2)$$

$\tilde{J}_\pm \equiv \tilde{J}_X \pm i \tilde{J}_Y$. The tilde indicates that the components of \vec{J} have been referred to a molecule-fixed coordinate frame. In Eq. (1), terms (4) and (5) form the Zeeman Hamiltonian W_Z ; terms (6) and (7) form the spin-rotation interaction W_{sr} ; and term (8) forms the spin-spin interaction. $O_{\text{dist}}^{(4)}$, O_{sr} , and O_{ss} are defined⁹ explicitly in Refs. 3 and 4.

Most of the constants in Eq. (1) are known from previous experiments. The rotational¹⁰ constant $B_0 = 5.2412 \pm 0.0005 \text{ cm}^{-1}$. The proton⁵ g factor $g_I = 5.5855 \mu_N$; the rotational^{2,11} g factor $g_J = +(0.3133 \pm 0.0002) \mu_N$. The average spin-rotation^{2,12} constant $c_a = +10.4 \pm 0.1 \text{ kHz}$; the anisotropy c_d in the spin-rotation¹² matrix = $+18.5 \pm 0.4 \text{ kHz}$; the spin-spin coupling¹² constant $d = +20.9 \pm 0.3 \text{ kHz}$. From various measurements of the distortion constant D_T by high-resolution infrared and Raman spectroscopy,^{7,10} we estimate that

$D_T \approx 120$ kHz. No value for the distortion constant D_U is available in the literature.

In the high-field limit, the most convenient representation for calculating the eigenvalues of W is characterized by the quantum numbers¹³ $\Gamma \equiv (Im_I m_J \rho)$. m_I and m_J are, respectively, the eigenvalues of I_Z and J_Z . ρ is a parity quantum number associated with the operator P which inverts the molecule-fixed reference frame. If $\rho = 1$, the totally symmetric inversion function is used. If $\rho = 2$, the totally antisymmetric inversion function is used. The basis functions in the Γ representation fall into three groups which can be written $\Psi(I=1, m_I, m_J, \rho=2)$, $\Psi(0, 0, m_J, 2)$, and $\Psi(0, 0, m_J, 1)$. The fact that the total wave function must be antisymmetric under the interchange of any two protons restricts I to the values 1 and 0 when $J=2$, and allows only the particular combinations of I and ρ indicated here. There are 25 levels in all.¹⁴

In the Γ representation, for $H \gtrsim 100$ G, the diagonal matrix elements arising from $D_T O_{\text{dist}}^{(4)}$ and W_Z are the largest terms (in magnitude)¹⁵ in the Hamiltonian matrix. If we indicate the diagonal matrix elements of W by $W(\Gamma)$, then

$$W(1, m_I, m_J, 2) \approx 24D_T - (g_I m_I + g_J m_J) \mu_N H / h, \quad (3)$$

$$W(0, 0, m_J, \rho) \approx -36D_T - (g_J m_J) \mu_N H / h. \quad (4)$$

Two types of off-diagonal matrix elements must be considered. The first arises from $-\frac{1}{3}c_d O_{\text{sr}}$. This is of the form $A_{\text{off}} \equiv \langle 1, m_I, m_J, 2 | W | 0, 0, m_I + m_J, 2 \rangle$, which is off-diagonal in I and will mix $\Psi(1, m_I, m_J, 2)$ and $\Psi(0, 0, m_I + m_J, 2)$.¹⁶ To see whether this mixing is significant, A_{off} must be compared with

$$A_{\text{diff}} \equiv W(1, m_I, m_J, 2) - W(0, 0, m_I + m_J, 2), \quad (5)$$

$$\approx 60D_T - (g_I - g_J) m_I \mu_N H / h. \quad (6)$$

Since $D_T > 0$, $A_{\text{diff}} \approx 0$ for $m_I = 1$ when $H = H_{\text{cr}}$, the "crossing" field defined by

$$H_{\text{cr}} = 60D_T [(g_I - g_J) \mu_N / h]^{-1}. \quad (7)$$

For $H \approx H_{\text{cr}}$, $|A_{\text{off}}| \geq |A_{\text{diff}}|$ and I cannot be treated as a good quantum number.

On the other hand, when H is not $\approx H_{\text{cr}}$, I is a good quantum number. For the value of c_d quoted above, $|A_{\text{off}}| \lesssim 20$ kHz. As $H \rightarrow 0$, $|A_{\text{diff}}| \rightarrow 60D_T$. As $H \rightarrow \infty$, $|A_{\text{diff}}| \rightarrow (g_I - g_J) \mu_N H / h$ if $m_I = \pm 1$, and $|A_{\text{diff}}| = 60D_T$ if $m_I = 0$. Since $60D_T \approx 8$ MHz, $|A_{\text{off}}| \ll |A_{\text{diff}}|$ in both limits. In fact, except for an interval ≈ 100 G centered at H_{cr} , $|A_{\text{off}}| \ll |A_{\text{diff}}|$, and the mixing caused by A_{off} is so

small as to be negligible in most problems. It is clear that, if $D_T = 0$, I would not be a good quantum number (even to first order) for any value of H .

The second type of off-diagonal matrix elements arises from $-D_U O_{\text{dist}}^{(3)}$. This is of the form $B_{\text{off}} \equiv \langle 0, 0, m_J, 2 | W | 0, 0, m_J, 1 \rangle$, which is off-diagonal in ρ , and will mix $\Psi(0, 0, m_J, 2)$ and $\Psi(0, 0, m_J, 1)$. W and P do not commute, a result directly related to the fact that CH_4 does not have a center of inversion. Since $[W(0, 0, m_J, 2) - W(0, 0, m_J, 1)] \equiv 0$, ρ is not a good quantum number (even to first order) for any H , regardless of how small D_U is, so long as $D_U \neq 0$.

Because the quantum numbers $\Gamma \equiv (Im_I m_J \rho)$ do not unambiguously identify the energy levels, we introduce a second representation $\Lambda \equiv (\lambda m)$.¹³ This is based on the artificial index λ which can take integral values from 1 to 5, and the only two physically significant quantum numbers which remain "good" for all H of interest, namely J and $m \equiv m_I + m_J$. The eigenvalues and eigenvectors of W can now be written $E(\lambda m)$ and $\varphi(\lambda m)$, respectively. As $H \rightarrow \infty$,

$$\Phi(1, m) \rightarrow \Psi(1, 1, m_J, 2), \quad (8a)$$

$$\Phi(2, m) \rightarrow (1/\sqrt{2})[\Psi(0, 0, m_J + 1, 2) + \epsilon \Psi(0, 0, m_J + 1, 1)], \quad (8b)$$

$$\Phi(3, m) \rightarrow (1/\sqrt{2})[\Psi(0, 0, m_J + 1, 2) - \epsilon \Psi(0, 0, m_J + 1, 1)], \quad (8c)$$

$$\Phi(4, m) \rightarrow \Psi(1, 0, m_J + 1, 2), \quad (8d)$$

$$\Phi(5, m) \rightarrow \Psi(1, -1, m_J + 2, 2). \quad (8e)$$

$\epsilon = +1$ if $D_U > 0$, and $\epsilon = -1$ if $D_U < 0$. The correspondence¹⁶ given in Eq. (8) serves to define λ . It is constructed so that $E(\lambda m) < E(\lambda' m')$ if $\lambda < \lambda'$. Not all values of λ are allowed for given m . For example, for $m = +3$, λ can equal only 1, since the other values of λ would require values of $m_J > J$.

By using the methods discussed in Refs. 2-4, the complete Hamiltonian matrix was calculated. A computer program was written which, for given D_T , D_U , and H , evaluates the $E(\lambda m)$ and the transition frequencies $\nu(\lambda m; \lambda' m')$ of interest. In Fig. 1, $E(\lambda m)$ is plotted against H for $\lambda = 1, 2$, and 3, and $m = 0$ and $+1$. In this plot, $D_T = 132.0$ kHz and $D_U = 1.6$ kHz.¹⁷ The value of "crossing" field H_{cr} is indicated. For both $m = 0$ and $+1$, as H decreases from H_{cr} , it can be seen from Fig. 1 that¹⁶ $\Phi(1, m) \rightarrow (1/\sqrt{2})[\Psi(0, 0, m_J + 1, 2) + \epsilon \Psi(0, 0, m_J + 1, 1)]$, $\Phi(2, m) \rightarrow (1/\sqrt{2})[\Psi(0, 0, m_J + 1, 2)$

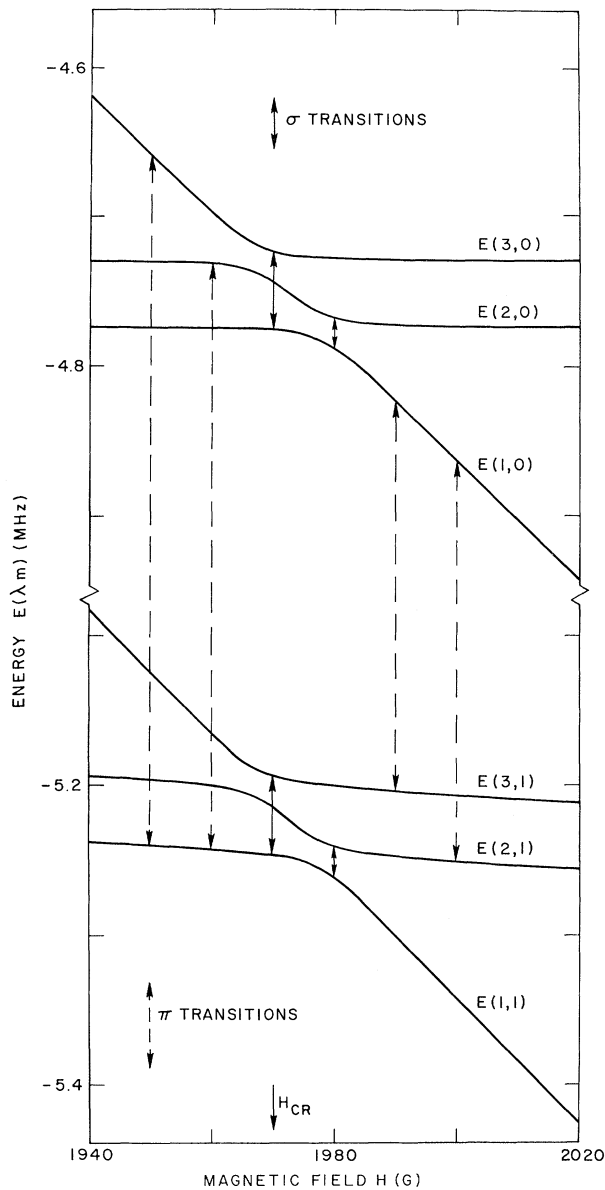


FIG. 1. Plot of energy $E(\lambda m)$ as a function of magnetic field H for $H \approx H_{cr}$, the "crossing" field defined in Eq. (7). The $m=0$ and $m=1$ levels are shown for $\lambda=1, 2$, and 3 . The ortho-para transitions possible among these six states are indicated. In the interest of clarity, the arrows used for this purpose are not all shown at the same field. The curves were calculated for $D_T=132.0$ kHz and $D_U=1.6$ kHz (see footnote 17).

$-\epsilon\Psi(0, 0, m_J+1, 1)$], and $\Phi(3, m) - \Psi(1, 1, m_J, 2)$. This correspondence is to be contrasted with that in Eq. (8) for $H \rightarrow \infty$.

However, for $H \approx H_{cr}$, the eigenvectors of W are a superposition of $\Psi(1, 1, m_J, 2)$, $\Psi(0, 0, m_J=1, 2)$, and $\Psi(0, 0, m_J+1, 1)$. As a result, all

magnetic dipole transitions $|\lambda m\rangle \leftrightarrow |\lambda' m'\rangle$ where $\Delta m = \pm 1$ or 0 are "allowed," although the number of ampere turns $NI_{opt}(\lambda m; \lambda' m')$ required to optimize the transition probability may be large. Those transitions where λ changes from $1, 4$, or 5 to 2 or 3 are of the ortho-para or " ΔI " type. The particular ΔI transitions of interest here are $|1m\rangle \leftrightarrow |2m'\rangle$ and $|1m\rangle \leftrightarrow |3m'\rangle$.

A search for the ortho-para transitions was made using a molecular-beam magnetic-resonance spectrometer.¹⁸ Prior to the detailed analysis, it was assumed that NI_{opt} for both π and σ transitions would be very large even for $H \approx H_{cr}$. This assumption led to the search being conducted in the following manner. The oscillating current I_{os} was passed through a solenoid consisting of two layers of 200 turns each connected in series. The solenoid was aligned with its axis nominally in the X direction (i.e., perpendicular to \vec{H}) to induce π transitions. Typically $NI_{os} \approx 1100$ A turns, so that the amplitude of the oscillating magnetic field generated ≈ 100 G. The static field H was set to a particular value, and then the frequency of I_{os} was swept from 1 to 45 kHz. Then H was changed slightly, and the frequency scan was repeated.

In this manner, H was varied from 1631 to 2252 G. A series of lines was observed for each of nine values of H between 1962.4 and 1992.1 G, and no lines were observed outside this region. The data¹⁹ are summarized in Fig. 2. A typical scan¹⁹ of the two lines observed for $H = 1971.5$ G is shown in Fig. 3.

These data have two major features. First, there are eight lines for $H = 1979.2$ G and six for $H = 1981.1$ G. Second, for each H between 1962.4 and 1992.1 G, there are two lines separated by ≈ 4 kHz. If we assume these lines always correspond to the same two transitions, then each of the two g factors $\approx 1.8\mu_N$ in magnitude. Unfortunately it is not possible, on the basis of the experimental data alone, to make any definite statements concerning the correspondence of the lines observed in one field with those observed in another. NI_{opt} was measured for several lines and, in each case, appeared to be 1100 A turns.

One final experimental test was performed. On the basis of the analysis presented here, the low frequency transitions observed can involve molecules which pass through the A deflecting magnet⁵ (where the field is $\gg H_{cr}$) in state $\Phi(1, 1, m_J, 2)$, but cannot involve those which pass through the A magnet in state $\Phi(1, -1, m_J, 2)$. For several lines, this prediction was checked

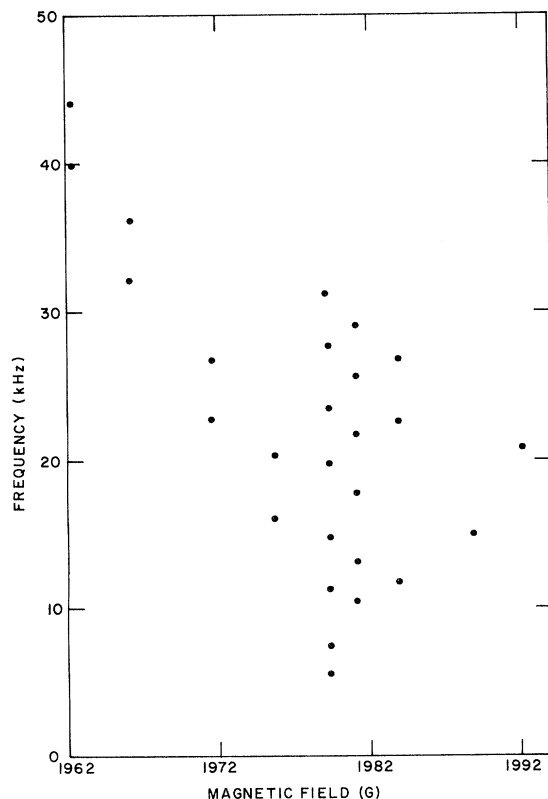


FIG. 2. Summary of the data. A point is plotted at each (frequency, field) position for which a line was observed (see footnote 19). The experimental error in the frequencies ≤ 500 Hz, while that in the fields ≤ 0.1 G.

experimentally by inserting an obstacle into the beam,²⁰ and was found to be correct.

The first attempt to fit the spectrum by varying D_T and D_U was made on the assumption that $\Delta m = \pm 1$ transitions had been observed. However, we were unable to obtain any qualitative agreement whatsoever between the theoretical frequencies and the data in Fig. 2. Furthermore, whenever the predicted frequencies were below 45 kHz, the corresponding calculated values of NI_{opt} were at least a factor of 10 larger than the 1100 A turns used in the experiment.

A second attempt to fit the spectrum was made on the assumption that σ transitions had been observed. In this case, NI_{opt} was calculated to be ≤ 20 A turns in certain regions of the (D_T, D_U) plane. If the angle between the effective solenoid axis and \vec{H} is $90^\circ - \theta$, then θ need be only $\leq 1^\circ$ for the 1100 A turns used in the experiment to optimize the probability of the σ transitions for these regions of the (D_T, D_U) plane. An angle of this size is quite reasonable. In the vicinity of the point $D_T = 132.0$ kHz and $D_U = 1.6$ kHz, a qualita-

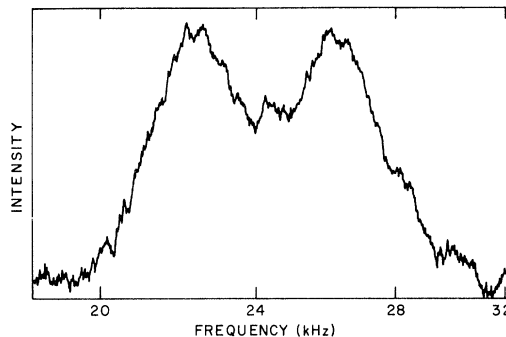


FIG. 3. The CH_4 ortho-para spectrum observed for $H = 1971.5$ G (see footnote 19).

tive fit to the data was obtained, except that it was not possible to reproduce the multiplicity of lines observed for $H = 1979.2$ and 1981.1 G. It is felt that the spectrum observed arose primarily from σ transitions, but was complicated by multiple-quantum transitions and frequency-pulling effects.

Equation (1) contains all the relevant⁸ terms whose existence has been previously established for CH_4 in the literature.^{1-3,5,7} Furthermore, on the basis of Eq. (1), a whole series of CH_4 spectra have been explained.^{2-4,11,12} Nevertheless, without a detailed identification of the individual lines, we cannot rule out the possibility that a term has been omitted from W . Moreover, we cannot assign definite values to D_U and D_T . However, the present best estimate for D_T (132.0 kHz) is in good agreement with the infrared and Raman values.^{7,10} The latter results are accurate only to $\geq 30\%$, whereas the method described here is inherently capable of determining D_T to $\leq 0.1\%$.

It is commonly assumed that, for all practical purposes, the two inversion levels of CH_4 are degenerate. It should be emphasized that the splitting between these levels has been resolved in the present experiment. Even if $D_U = 0$, the two inversion levels are split by a few kilohertz in the crossing region. A detailed treatment of the inversion process may be necessary to explain the spectra observed here.

A second experiment is planned in which the solenoid axis will be in the Z direction and $I_{\text{os}} \approx 10$ A turns. These changes will simplify both the spectrum and the analysis. Ultimately the ortho-para spectrum of CH_4 should provide not only accurate values of D_T and D_U , but also independent measurements of g_J , c_a , c_d , and d , and (with modest improvements in the apparatus) the first determination of the anisotropy in the

magnetic shielding tensor. While CH_4 is particularly suited to this technique, it can be applied to other tetrahedral molecules, such as CD_4 and SiH_4 , where $60D_T \gg c_d$.

We thank Dr. K. Fox and Dr. K. W. Gray for many helpful discussions.

*Work supported in part by the National Science Foundation and the U. S. Office of Naval Research.

†Present address: De Paul University, Chicago, Ill.

¹G. Herzberg, Infrared and Raman Spectra of Polyatomic Molecules (Van Nostrand, Princeton, N. J., 1945).

²C. H. Anderson and N. F. Ramsey, *Phys. Rev.* **149**, 14 (1966).

³P. N. Yi, I. Ozier, and C. H. Anderson, *Phys. Rev.* **165**, 92 (1968).

⁴I. Ozier, L. M. Crapo, and S. S. Lee, *Phys. Rev.* **172**, 63 (1968).

⁵N. F. Ramsey, Molecular Beams (Oxford Univ., Oxford, England, 1956).

⁶For a review of these studies, see K. P. Wong, J. D. Noble, M. Bloom, and S. Alexander, *J. Mag. Res.* **1**, 55 (1969).

⁷K. T. Hect, *J. Mol. Spectry.* **5**, 355, 390 (1960).

⁸Equation (1) omits the nuclear shielding terms, the scalar electron-coupled spin-spin interaction, and a rotational-distortion term which depends only on J . All three of these can be neglected here.

⁹ $D_T O_{\text{dist}}^{(4)} = W_{\text{dist}}$ of Ref. 3. $O_{ss} = O_{ss}^E + O_{ss}^T$ of Ref. 4.

¹⁰J. Herranz and B. P. Stoicheff, *J. Mol. Spectry.* **10**, 448 (1963); R. S. McDowell, *ibid.* **21**, 280 (1966). $D^J \tau / 10$ (as defined in these two works) equals D_T (as defined in Ref. 7 and used here).

¹¹I. Ozier, S. S. Lee, and N. F. Ramsey, to be published. The sign of g_J was determined in this work.

¹²P. N. Yi, thesis, Harvard University, 1967 (unpublished).

¹³Since the entire discussion deals only with the $J=2$ rotational level, J is not explicitly included in the list of quantum numbers.

¹⁴Detailed discussions of the Γ representation and the wave functions are given in Ref. 3 and in I. Ozier and K. Fox, to be published. However, both of these works state, incorrectly, that ρ is associated with the inversion of the space-fixed reference frame. In both cases, ρ should be associated with the inversion of the molecule-fixed reference frame, as is done here.

¹⁵It is assumed here that $|D_U| < |D_T|$. This was subsequently found to be the case experimentally.

¹⁶Notice that the values of m_I and m_J have been so specified that $m \equiv m_I + m_J$ is conserved.

¹⁷The sign of D_U is not significant here because the spectrum depends only on the magnitude of this constant.

¹⁸The apparatus used is described in M. R. Baker, H. M. Nelson, J. A. Leavitt, and N. F. Ramsey, *Phys. Rev.* **121**, 807 (1961).

¹⁹Because an oscillating rf field was used rather than a rotating one, only the absolute value of the frequency observed is significant.

²⁰A detailed description of the method used is given in I. Ozier, L. M. Crapo, and N. F. Ramsey, *J. Chem. Phys.* **49**, 2314 (1968).

LONG-WAVELENGTH PHONONS IN LIQUID HELIUM

A. D. B. Woods and R. A. Cowley

Atomic Energy of Canada Limited, Chalk River, Ontario, Canada

(Received 6 January 1970)

High-resolution neutron-scattering measurements have been made of long-wavelength-phonon energies $\hbar\omega$ in liquid helium at 1.1°K as a function of wave vector Q . The results are approximately described by $\omega = cQ(1 - \gamma\hbar^2 Q^2 - \delta\hbar^4 Q^4)$, with γ very small ($< 2 \times 10^{36} \text{ g}^{-2} \text{ cm}^{-2} \text{ sec}^2$) and $\delta = (2.4 \pm 0.2) \times 10^{75} \text{ g}^{-4} \text{ cm}^{-4} \text{ sec}^4$.

Inelastic neutron-scattering measurements of the energies $\hbar\omega$ of long-wavelength phonons in liquid helium at 1.1°K have been carried out for wave vectors $Q \geq 0.2 \text{ \AA}^{-1}$ (phonon momentum $p = \hbar Q$). The results show that the phonon velocity exhibits remarkably little dispersion for $Q \leq 0.5 \text{ \AA}^{-1}$, that the term in Q^3 in the expression for the phonon energies is very small, and that the term in Q^5 represents a more accurate description of the observed dispersion. This result has important consequences for the calculation of other properties of liquid helium such as the ultrasonic attenuation at low temperatures.

It may possibly help to resolve the present discrepancy between such calculations and the observed¹ attenuation. The intensities of the one-phonon neutron groups are linear in Q and, within the limits of the experimental accuracy, exhaust the f sum rule² for $Q \leq 0.3 \text{ \AA}^{-1}$, but not for larger wave vectors.

If the long-wavelength-phonon energies are given by the expression

$$k_B \epsilon \equiv \hbar\omega = cp(1 - \gamma p^2 - \delta p^4 + \dots) \\ = \hbar cQ(1 - \gamma \hbar^2 Q^2 - \delta \hbar^4 Q^4 + \dots),$$